DINAME 2023 - Proceedings of the XIX International Symposium on Dynamic Problems of Mechanics,
A.S. De Paula, A.T. Fabro and M.R. Machado (Editors), ABCM.
Pirenópolis, Go, Brazil, February 26th to March 3rd, 2023

Application of Kalman Filter as a Method to Balance Rotors without Trial Masses

Fabio Dalmazzo Sanches [1], Aldemir Aparecido Cavallini Junior [2]

[1] Universidade Federal do Rio Grande do Norte. Avenida Senador Salgado Filho, 3000. Campus Universitário Lagoa Nova – Centro de Tecnologia, departamento de Engenharia Mecânica, Natal-RN, CEP: 59078-900.

[2] Universidade Federal de Uberlândia. Avenida João Naves de Ávila, 2121 – Laboratório de Mecânica de Estruturas "Prof. José Eduardo Tannus Reis, bloco 1O/SM, Santa Mônica, Uberlândia-MG, CEP: 38400-902.

Abstract: This paper focuses on an ancient problem in rotating machines: unbalance. The presence of rotor mass imbalance is due to eccentricity of the mass centroidal axis of the rotor relative to its axis of rotation and is a result of unavoidable imperfections in rotor manufacture and assembly. To produce a smooth-running machine, procedures to balance the rotor must be employed. Kalman filtering is an algorithm that provides estimates of some unknown variables given the measurements observed over time and it was originally formulated to estimate the states of a dynamic system. The augmented Kalman (AKF) filter includes the inputs (forces) as variables to be determine together with the states. This paper studies the feasibility of AKF to estimate the unbalance forces and, consequently, be a procedure to balance a rotating machine, since no trial masses are required. The studies are performed theoretically considering different unbalance configurations and considering noise in the rotor responses. The methodology proved to be efficient to estimate the unbalance forces and some care must be taken when experimental tests are carried out, as noise has been shown to be an important aspect for the accuracy of the method.

Keywords: balancing, Kalman filter, rotor dynamics

INTRODUCTION

Unbalance is the most common cause of excessive vibration in rotating machines, causing large forces on the bearing supports. This may cause the fatal failure of mechanical components such as bearings and couplings. Wowk (1995) highlights some reasons to balance a machine since low vibration: minimizes noise, increases bearing life, decreases operating stresses, consumes less energy, increases product quality, decreases operator fatigue, eliminates fatigue failures of support structures and satisfies customers.

Tiwari and Kumar (2022) proposed a model-based algorithm derived from virtual trial misalignment to identify the rotor unbalance, active magnetic bearings (AMBs) residual misalignment and their displacement and current stiffness parameters. Li *et al.* (2022) prosed an unbalance identification method for full-size large rotor systems such as aero-engines and gas turbines by using scaling laws and scaled model. Da Silva and Pederiva (2019) identified the unbalance using correlation equations through the matrix formulation of Ljapunov for stationary linear systems along with artificial neural networks.

A Kalman filter is an optimal recursive data processing algorithm that incorporates all information that can be provided to it, processing all available measurements, regardless of their precision, to estimate the current values of the variables of interest, using: (1) knowledge of the system and measuring device dynamics; (2) the statistical description of the system noises, measurement errors and uncertainty in the dynamic models; and (3) any available information about initial conditions of the variables of interest (Maybeck, 1979). This algorithm is used to estimate the system states as well as the model parameters (Aguirre, 2007).

Considering the system inputs, Lourens *et al.* (2012) prosed an augmented Kalman filter (AKF) technique for dynamic force identification in a combined deterministic-stochastic setting. Shrivastava and Mohanty (2018) used the the AKF to identify the unbalance in a single plane rotor. Zou *et al.* (2019) proposed the usage of AKF to balance a simple isotropic rotor. This paper improves the work done by Zou *et al.* (2019) considering an anisotropic rotor as well the coupling parameters and a higher number of degrees of freedom. The methodology proved to be effective as a method to balance a rotor without trial masses and, consequently, enhancing the machine availability.

MATHEMATICAL MODELING

Considering the rotor system, which contains *f* unbalance forces, a linear time invariant system of order *n*, it can be described by the differential matrix equation:

$$\mathbf{M}\ddot{\mathbf{u}}(t)+\mathbf{P}\dot{\mathbf{u}}(t)+\mathbf{K}\,\mathbf{u}(t)=\mathbf{f}(t)=\mathbf{S}_p\mathbf{p}(t) \tag{1}$$

where **M, P** and **K** are the mass, damping and stiffness matrices respectively; **f** is a vector of forces, $\mathbf{S_P}$ is a matrix that locates the unbalance forces and has order (*n,f*) and **p** is a vector of order (*f*,1) that represents the rotor unbalances.

The system described by Eq. (1) can be written in the expanded state space representation, in which the inputs (forces) is part of the state vector:

$$\dot{\mathbf{x}}_e(t) = \mathbf{A}_e\mathbf{x}_e(t) \tag{2}$$

$$\mathbf{y}_e(t) = \mathbf{C}\mathbf{x}_e(t) \tag{3}$$

Subscript *e* indicates the expanded system. The expanded state vector has the following structure:

$$\mathbf{x}_e = \begin{bmatrix}\mathbf{u}(t) & \dot{\mathbf{u}}(t) & \mathbf{p}(t)\end{bmatrix}^T \tag{4}$$

The expanded system matrix is written as

$$\mathbf{A}_e = \begin{bmatrix} \mathbf{0}_{(n,n)} & \mathbf{I}_{(n,n)} & \mathbf{0}_{(n,f)} \\ -\mathbf{M}^{-1}\mathbf{K} & -\mathbf{M}^{-1}\mathbf{C} & \mathbf{M}^{-1}\mathbf{S}_P \\ \mathbf{0}_{(f,n)} & \mathbf{0}_{(f,n)} & \mathbf{\Gamma}_{(f,f)} \end{bmatrix} \tag{5}$$

$\mathbf{\Gamma}$ is a matrix that transforms the unbalance force vector of the global system into $\dot{\mathbf{p}}(t)$:

$$\mathbf{\Gamma} = \begin{bmatrix} 0 & \Omega \\ -\Omega & 0 \end{bmatrix} \tag{6}$$

where Ω is the rotor rotating speed.

The Eqs. (2) and (3) can be written discrete form:

$$\mathbf{x}_{k+1} = \mathbf{\Phi}\mathbf{x}_k + \begin{bmatrix}\mathbf{w}_k & \mathbf{\eta}_k\end{bmatrix}^T \tag{7}$$

$$\mathbf{y}_k = \mathbf{G}_a\mathbf{x}_k + \mathbf{\nu}_k \tag{8}$$

$\mathbf{\Phi}$ is the system matrix, $\mathbf{G}_a = \mathbf{C}$, $\mathbf{w}_k$ and $\mathbf{\eta}_k$ are the random noise vectors of the system model and the unbalance forces, respectively. $\mathbf{\nu}_k$ is the random noise associated to the rotor outputs (measurements). All the noise processes are assumed to be stationary, mutually uncorrelated stochastic processes with zero mean. Their covariances are assumed known and are represented by matrices:

$$E\left\{\mathbf{w}_k\mathbf{w}_l^T\right\} = \mathbf{Q}\delta_{k-l} \tag{9}$$

$$E\left\{\mathbf{\nu}_k\mathbf{\nu}_l^T\right\} = \mathbf{R}\delta_{k-l} \tag{10}$$

$$E\left\{\mathbf{\eta}_k\mathbf{\eta}_l^T\right\} = \mathbf{S}\delta_{k-l} \tag{11}$$

where δ_{k-l} is the Kronecker delta.

The Kalman filter equations for the discrete-time system of Eqs. (7) and (8) are (Lourens *et al.*, 2012):

Measurement update:

$$\mathbf{L}_k = \mathbf{P}_{k/k-1}\mathbf{G}_a^T\left(\mathbf{G}_a\mathbf{P}_{k/k-1}\mathbf{G}_a^T + \mathbf{R}\right)^{-1} \tag{12}$$

$$\hat{\mathbf{x}}_{k/k} = \hat{\mathbf{x}}_{k/k-1} + \mathbf{L}_k\left(\mathbf{y}_k - \mathbf{G}_a\hat{\mathbf{x}}_{k/k-1}\right) \tag{13}$$

$$\mathbf{P}_{k/k} = \mathbf{P}_{k/k-1} - \mathbf{L}_k\mathbf{G}_a\mathbf{P}_{k/k-1} \tag{14}$$

Time update:

$$\hat{\mathbf{x}}_{k+1/k} = \mathbf{\Phi}\hat{\mathbf{x}}_{k/k} \tag{15}$$

$$\mathbf{P}_{k+1/k} = \mathbf{\Phi}\mathbf{P}_{k/k}\mathbf{\Phi}^T + \mathbf{Q}_a \tag{16}$$

$\mathbf{Q}_a$ is the augmented covariance matrix:

$$\mathbf{Q}_a = \begin{bmatrix} \mathbf{Q} & \mathbf{0} \\ \mathbf{0} & \mathbf{S} \end{bmatrix} \tag{17}$$

TEST RIG DESCRIPTION

The numerical results are performed in the test rig showed by Fig.1:

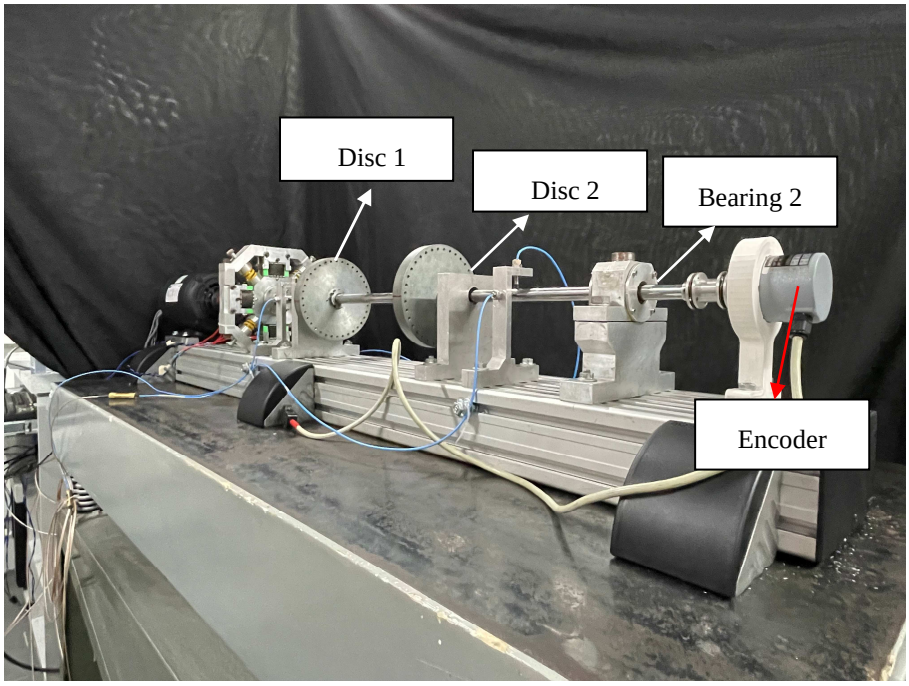

Figure 1 – Test rig

The test rig has the characteristics showed by Tab.1:

Table 1 – Test rig characteristics

Properties	Shaft	Disc 1	Disc 2
Length (m)	1.00	----	----
Diameter (m)	17e-3	150e-3 (outer)	150e-3 (outer)
Mass (kg)	----	2.587	2.601
Width (m)	----	20e-3	20e-3
Material	Steel 1045	Steel 1020	Steel 1020
Poisson's ratio	0.297109	----	----
Modulus of elasticity (GPa)	211.2959	----	----
Density (kg/m^3)	7800	----	----

The rotor is modeled by finite elements with of 39 nodes and 156 degrees of freedom, the discs are mounted at nodes #14 (disc 1) and #25 (disc 2) supported by two rolling bearings FAG 1204-K-TVH-C3 located at nodes #5 (bearing 1) and #36 (bearing 2).

Some important properties that have strong influence on the rotor dynamic behavior such as bearing and coupling parameters, as well as the structural proportional damping coefficients, were determined using Differential Evolution method (Storn and Price, 1995) to fit the simulated frequency response functions (FRF) with the experimental ones acquired with an impact hammer considering the input at the discs' position and the outputs at nodes #8 (sensor 1) and #31 (sensor 2). Figure 2 shows the result of the optimization process and Table 2 shows the optimized parameters in which subscript *x* and *z* represents the directions horizontal and vertical respectively.

With the rotor parameters in Tab.2, the rotor model is considered accurate, so the matrix is null. Lourens *et al.* (2012) suggest assigning large values to the diagonal of the matrix **S** to treat the initial errors as large and cause the filter to ignore the initial estimations, the chosen value was 1e8. Naets, Cuadrado and Desmet (2015) affirm the matrix **R** should chosen an order of magnitude higher than the systems responses, so the used diagonal terms are equal to 1e-5.

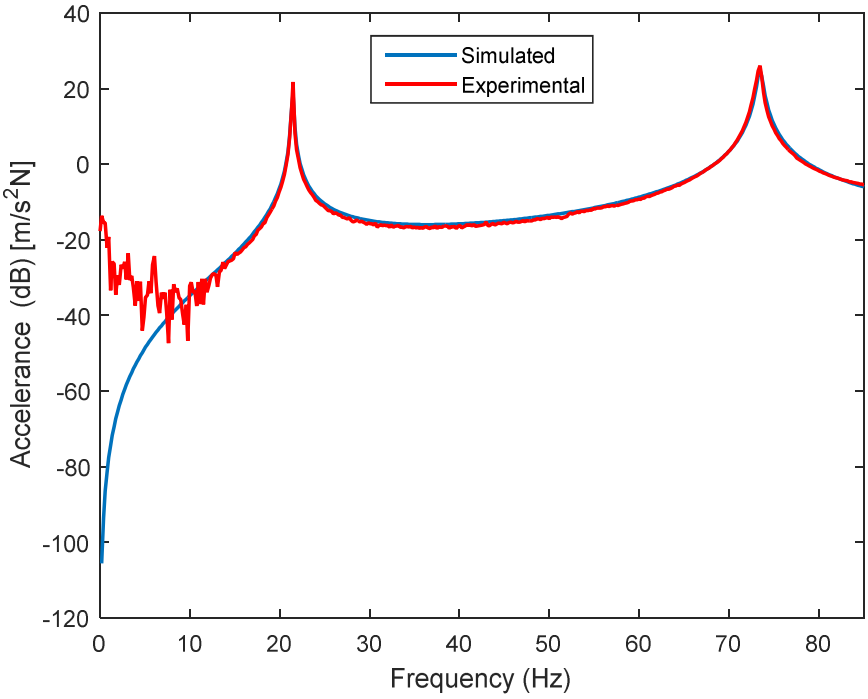

Figure 2 – FRF input disc 2, output sensor 1: horizontal direction

Table 2 – Adjusted parameters

Bearing 1	Value
k_x	5.42132e5 N/m
k_z	1.545597e6 N/m
c_x	3.337769e1 Ns/m
c_z	2.923775 Ns/m
Bearing 2	
k_x	7.814679e9 N/m
k_z	1.00e7 N/m
c_x	1.079132e2 Ns/m
c_z	2.923775 Ns/m
Coupling	
K	1.392289e3 Nm/rad
Proportional structural damping	
α	7.587876e-1
β	4.31026e-6

NUMERICAL RESULTS

The simulations consider the discs as the only sources causing vibrations in the machine due to independent unbalances (*inputs*). Since in a real machine the discs' position are not used to acquire the rotor responses, the *output* signals, which are the displacements at the directions horizontal and vertical, are taken at the positions of the discs.

The Kalman filter is tested considering five theoretical different configurations showed by Tab. 3:

Table 3 – Unbalance configurations

Configuration	Disc 1	Disc 2
C1	2.72e-4 kgm@35º	2.04e-4 kgm@70º
C2	2.72e-4 kgm@35º	2.04e-4 kgm@150º
C3	2.72e-4 kgm@35º	2.04e-4 kgm@240º
C4	2.72e-4 kgm@35º	2.04e-4 kgm@315º
C5	2.72e-4 kgm@150º	2.04e-4 kgm@150º

The total time of simulation is 20s and the sample rate is 2500Hz.

After performing the Kalman filter, the numerical results are depicted in Tab. 4:

Table 4 – Numerical results at disc´s position

Configuration	Disc 1	Disc 2
C1	2.7147e-4 kgm@38.5623º	2.03347e-4 kgm@73.6602º
C2	2.7182e-4 kgm@38.5446º	2.03384e-4 kgm@153.6973º
C3	2.7195e-4 kgm@38.6250º	2.03384e-4 kgm@243.5544º
C4	2.7164e-4 kgm@38.6568º	2.0362e-4 kgm@318.4924º
C5	2.7141e-4 kgm@318.5964º	2.0330e-4 kgm@318.5979º

Figures 3 shows the unbalance forces at both discs:

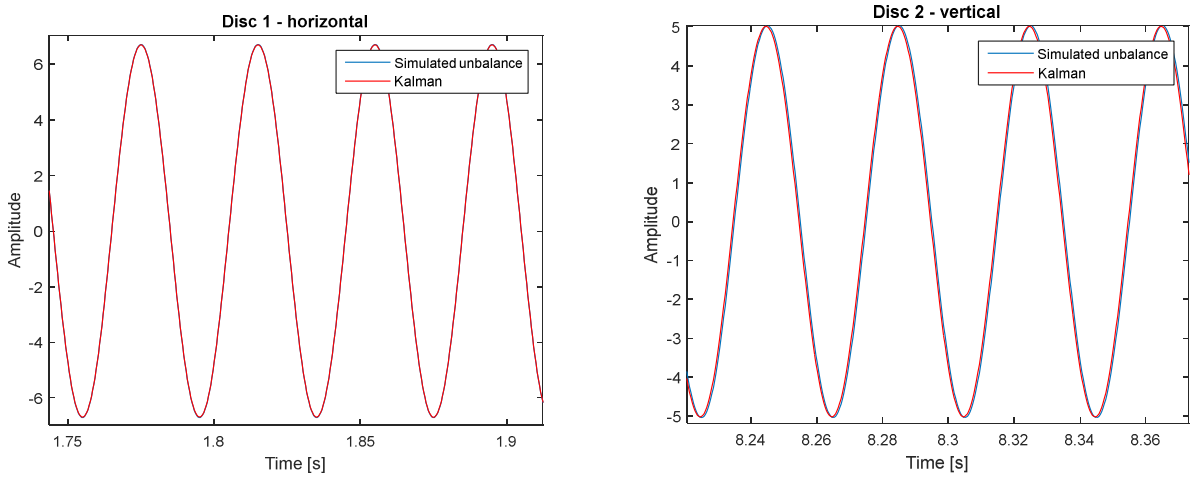

Figure 3 – Comparison between the true unbalance and Kalman estimation at disc´s position

It is possible to observe from Table 4 and Fig.3 that the Kalman filter can predict the unbalance forces with accuracy when the rotor responses do not have any noise in the machine signals, which is not correct in practical situations with real machines present in industries.

Simulations at shaft positions

Since the responses at the discs position are not acquired easily, simulations are performed considering the rotor responses at two nodes of the shaft different from the position of the discs.

The simulations consider two nodes near the discs ones, nodes #16 and #23, and the results are depicted in Table 5:

Table 5 – Numerical results with responses at nodes #16 and #23

Configuration	Disc 1	Disc 2
C1	2.7147e-4 kgm@38.5623º	2.0337e-4 kgm@73.6602º
C2	2.7182e-4 kgm@38.5446º	2.0384-4 kgm@153.6973º
C3	2.7195e-4 kgm@38.6250º	2.0403e-4 kgm@243.5544º
C4	2.7164e-4 kgm@38.6568º	2.0362e-4 kgm@318.4925º
C5	2.7141e-4 kgm@153.5964º	2.0330e-4 kgm@153.5979º

As one can see from Tab.5, when the rotor nodes outputs do not coincide with the nodes that generate the unbalance forces the identification continues as accurate as the ones showed by Tab.4. To verify if the results in Tab.5 can balance the rotor, comparisons between the original responses and the “Kalman balancing” are made and showed by Figs.4 and 5.

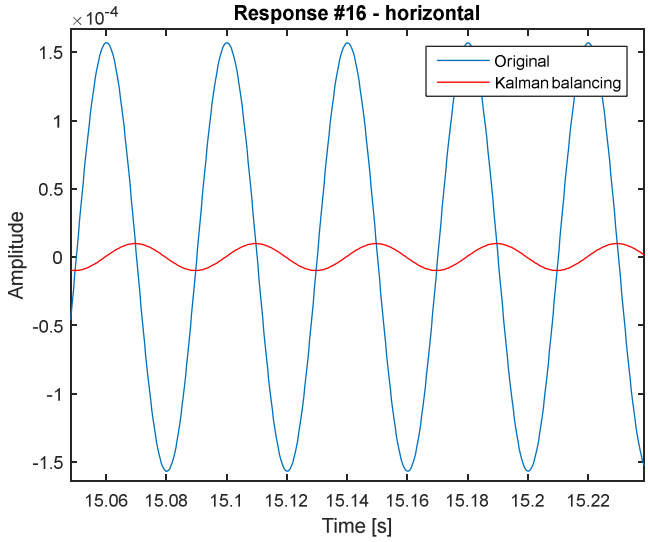

(a)

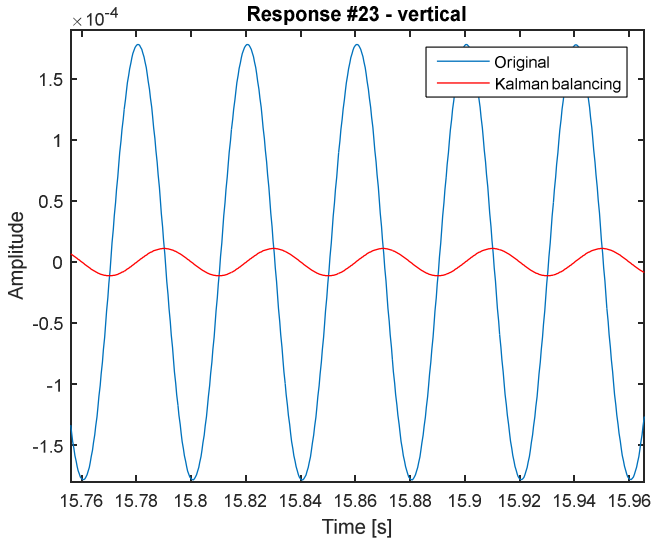

(b)

Figure 4 – Kalman balancing configuration C2: (a) node #16, (b) node #23

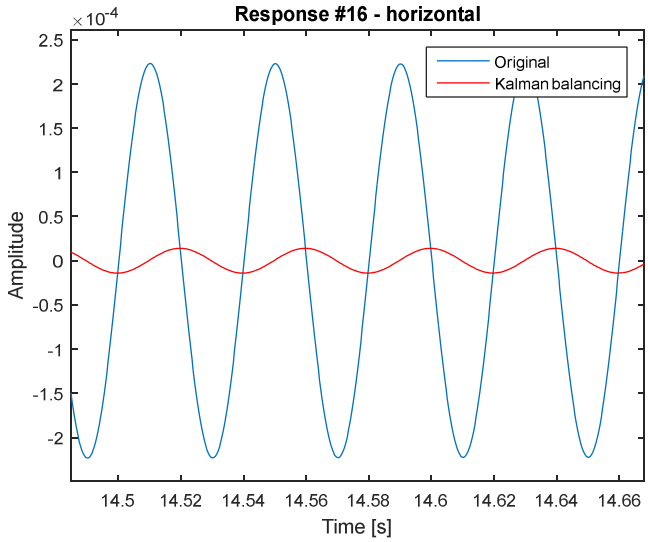

(a)

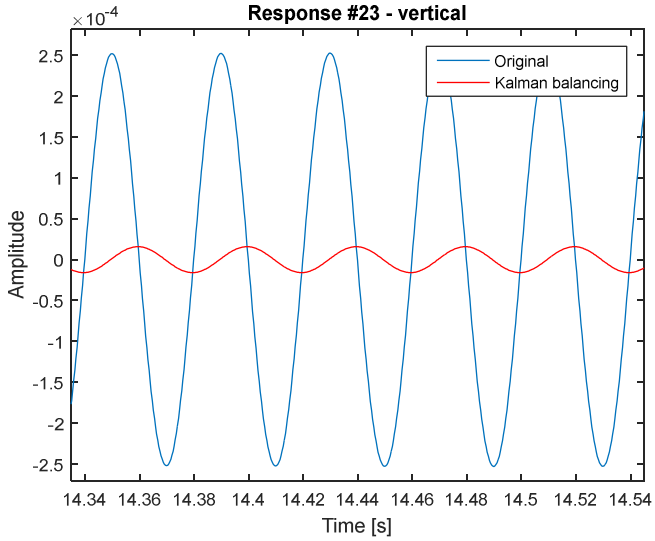

(b)

Figure 5 – Kalman balancing configuration C4: (a) node #16, (b) node #23

As one can see from Figs. 4 and 5 a reduction in vibration amplitude by 94%.

The same simulations in Tab.5 are made considering the vibration responses acquired at positions on the shaft furthest from the discs, the goal is to verify if the location of the sensors affects the estimates that Kalman filter produce. Nodes #8 and #31are chosen to generate the results, which are showed by Table 6.

Table 6 – Numerical results with responses at nodes #8 and #31

Configuration	Disc 1	Disc 2
C1	2.7147e-4 kgm@38.5624º	2.0336e-4 kgm@73.6601º
C2	2.7182e-4 kgm@38.5446º	2.0384-4 kgm@153.6973º
C3	2.7195e-4 kgm@38.6250º	2.0403e-4 kgm@243.5544º
C4	2.7164e-4 kgm@38.6568º	2.0362e-4 kgm@318.4922º
C5	2.7141e-4 kgm@153.5964º	2.0330e-4 kgm@153.5978º

It is possible to observe from Tab.6 that the results are practically the same as those shown in Tab. 5. It is interest to highlight that location of the measuring points is not important, the Kalman filter is able to estimate the unbalance forces at each disc.

Simulations with noise

To simulate a more real situation that occurs in experimental tests as well as field acquisitions, configuration C3 is simulated considering four signal-noise rates (SNR) and acquisition at the discs: 25, dB, 35 dB, 40 dB and 55 dB. Table 7 shows the results:

Table 7 – Numerical results with noise: discs position

SNR	Disc 1	Disc 2
25 dB	4.0077e-4 kgm@121.3559º	4.4121e-4 kgm@215.1220º
35 dB	2.8361e-4 kgm@45.0073º	2.3034e-4 kgm@241.9405º
40 dB	2.7583e-4 kgm@38.5788º	2.1224e-4 kgm@243.5853º
55 dB	2.7207e-4 kgm@38.6240º	2.0428e-4 kgm@243.5550º

One can see by the results showed in Tab. 7, the results with noise are worse than the ones without noise. This is an indication that some minimum SNR is necessary to balance the rotor satisfactorily or the measured signals should be filtered to remove high frequency components.

Table 8 depicts the results considering measurements at nodes #8 and #31considering noise. The purpose is to verify if the noise has stronger effects when the estimations are taken far from the discs.

Table 8 – Numerical results with noise: nodes #8 and #31

SNR	Disc 1	Disc 2
25 dB	3.0376e-4 kgm@71.7015º	2.9996e-4 kgm@230.1613º
35 dB	2.7846e-4 kgm@38.5885º	2.1270e-4 kgm@243.5026º
40 dB	2.7280e-4 kgm@38.6120º	2.0675e-4 kgm@243.5318º
55 dB	2.7197e-4 kgm@38.6239º	2.0411e-4 kgm@243.5539º

As one can compare Tabs. 7 and 8, the higher is the SNR the better are the results of the estimation. It is interesting to point out that the Kalman filter seems to be insensitive to the location of measurement points, which is very good for running experimental acquisitions.

EXPERIMENTAL RESULTS

The discs contain a total of 36 threaded holes at the diameter of 68 mm, with the 36th hole (0º or 360º) being the one that coincides with the encoder pulse. The first hole corresponds 10º marked in the direction of rotation of the test rig.

Table 9 shows the unbalance distribution placed for the discs, three masses were added in each disc.

Table 9 – Unbalance distribution at each disc

	Disc 1	Disc 2
Unbalance masses	3.83g@160º + 2.04g@180º + 3.5g@210º	3.43g@190º + 1.75g@200º + 3.42g@210º

The vibration signals were measured at nodes #8 and #31 for the rotational speed of 840 rpm (14 Hz). After using the experimental signals in the AKF algorithm the identified balancing masses were: 7.6g@348.4169º for the disc 1 and 4.3g@4.2728º for the disc 2. Table 10 shows the balancing masses and the true positions at each disc.

Table 10 – Unbalance distribution at each disc

	Identified mass	True mass
Disc 1	7.60g@348.4169º	7.66g@350.00º
Disc 2	4.30g@4.2728º	2.84g@0º + 1.36g@10º

Figures (6) and (7) show the comparison between the original unbalanced response caused by the unbalance masses showed by Tab.(9) and the balanced behavior after placing the balancing masses presented by Tab.(10).

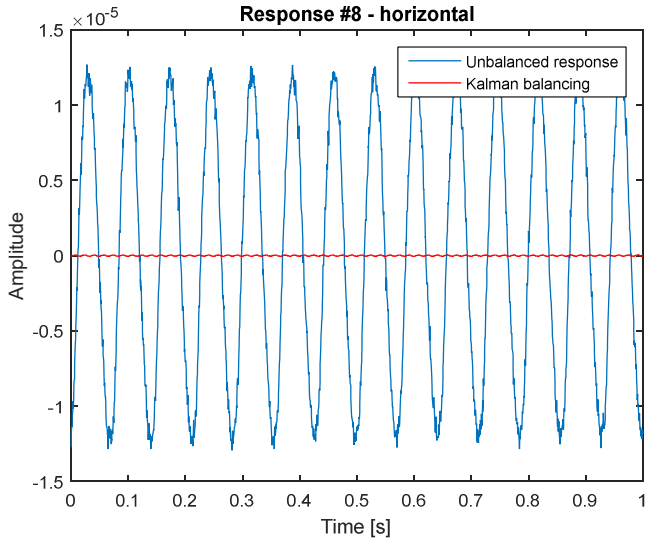

Figure 6 – Kalman balancing node #8

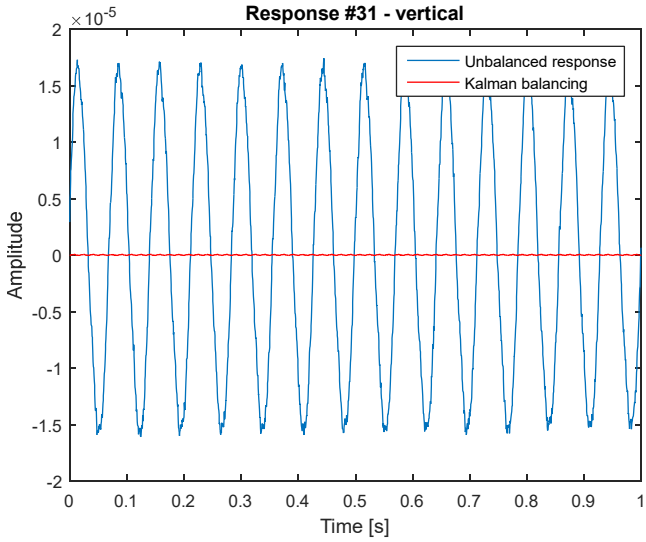

Figure 7 – Kalman balancing node #31

As one can see from Figs.(7) and (8), the balancing procedure was successful and the rotor vibration was strongly reduced.

CONCLUSIONS

The Kalman filter is a good methodology to balance rotors. Using only four measurements, in a total of 156 degrees of freedom, it was possible to identify and distinct unbalances at two different planes. As showed by Tabs. 7 and 8, care must be taken when real experiments are carried out since a minimum SNR is necessary.

The methodology proved to be effective both theoretically as well as experimentally and it is a good technique to be used in continuous monitoring, especially in critical equipment.

It is important to note that it is not necessary to stop the machine to estimate the correction masses to perform the balancing, reducing the time the machine is not operating and, consequently, financial losses.

REFERENCES

Aguirre, L.A., 2007, “Introdução à Identificação de Sistemas: Técnicas Lineares e Não-Lineares Aplicadas a Sistemas Reais”, Ed. UFMG, Belo Horizonte, Brasil, 728 p.

Da Silva, G. and Pederiva, R., 2019, “Unbalance Identification in a Rotor Supported by Active Magnetic Bearing”. In: Cavalca, K., Weber, H. (eds) Proceedings of the 10th International Conference on Rotor Dynamics – IFToMM. IFToMM 2018. Mechanisms and Machine Science, vol 60. Springer.

Li, L. *et al.*, 2022, “Experimental and Numerical Investigations on an Unbalance Identification Method for Full-Size Rotor System based on Scaled Model”, Journal of Sound and Vibration, Vol. 527, 116868.

Lourens *et al.*, 2012, “An Augmented Kalman Filter for Force Identification in Structural Dynamics”, Mechanical Systems and Signal Processing, Vol. 27, pp. 446-460.

Maybeck, P.S., 1979, “Stochastic Models, Estimation and Control: volume 1”, Ed. Academic Press, INC, Orlando, USA, 423 p.

Naets, F., Cuadrado, J., Desmet, W., 2015, “Stable force identification in structural dynamics using Kalman filtering and dummy-measurements”, Mechanical Systems and Signal Processing, Vol. 50-51, pp. 235-248.

Shrivastava, A., Mohanty, A. R., 2018, “Estimation of single plane unbalance parameters of a rotor-bearing system using Kalman filtering based force estimation technique”, Vol. 418, p. 184-199.

Storn, R., Price, K., 1995, “Differential Evolution: a simple and efficient adaptive scheme for global optimization over continuous spaces”. International Computer Science Institute, Vol. 12, n. 1, p. 1-16.

Tiwari, R., Kumar, P., 2022, “An Innovative Virtual Trial Misalignment Approach for Identification of Unbalance, Sensor and Active Magnetic Bearing Misalignment along with its Stiffness Parameters in a Magnetically Levitated Flexible Rotor System”, Mechanical Systems and Signal Processing, Vol. 167, Part A, 108540.

Wowk, V., 1995, “Machinery Vibration: Balancing”, Ed. McGraw-Hill, New York, United States, 322 p.

Zou *et.al.*, 2019, “Application of augmented Kalman filter to identify unbalance load of rotor-bearing system: Theory and experiment”, Journal of Sound and Vibration, Vol. 463, 114972.

RESPONSIBILITY NOTICE

The authors are the only responsible for the printed material included in this paper.